



Voltammetric determination of cadmium(II), lead(II) and copper(II) with a glassy carbon electrode modified with silver nanoparticles deposited on poly(1,8-diaminonaphthalene)

Khalid M. Hassan¹ · Ghada M. Elhaddad² · Magdi AbdelAzzem²

Received: 31 January 2019 / Accepted: 24 May 2019 / Published online: 13 June 2019
© Springer-Verlag GmbH Austria, part of Springer Nature 2019

Abstract

A glassy carbon (GC) electrode was modified with poly(1,8-diaminonaphthalene) (p-1,8-DAN) that was coated with silver nanoparticles (Ag NPs) (size: 10.0–60.0 nm by TEM) by electrodeposition process using cyclic voltammetry (CV) technique. The resulting nanocomposite was characterized by FE-SEM, AFM, EDX, XPS, TEM and XRD. The surface area and the electrochemical characteristics of the electrode were investigated by CV and square wave voltammetry (SWV) techniques, and the probe preparation conditions were optimized. The electrode was used for individual and simultaneous determination of the heavy metal ions cadmium(II) (Cd^{2+}), lead(II) (Pb^{2+}) and copper(II) (Cu^{2+}) in water samples by square wave anodic stripping voltammetry (ASV) using scan rate $0.005 \text{ V} \cdot \text{s}^{-1}$. The probe showed well separated anodic stripping peaks for Cd^{2+} , Pb^{2+} , and Cu^{2+} . Attractive features of the method include (a) peak voltages of -1.02 , -0.78 and -0.32 V (vs. Ag/AgCl) for the three ions, and (b) low limits of detection (19 , 30 and $6 \text{ ng} \cdot \text{L}^{-1}$, respectively). The electrode can also detect zinc(II) (Zn^{2+}) and mercury(II) (Hg^{2+}), typically at -1.36 V and $+0.9$, respectively.

Keywords Nanoprobe · Electrodeposition · Individual and simultaneous determination · Stripping anodic voltammetry

Introduction

One of the major involvement of the environmental pollution is heavy metals such as cadmium (Cd), lead (Pb) and Copper (Cu) owing to their contribution in different natural and industrial activities, and playing a vital role in numerous biological activities in organisms [1]. Different analytical techniques such as atomic absorption developed for determination of metal traces [2]. On the other hand, electrochem-

ical techniques, specifically electrochemical stripping technique were extensively proved to be suitable for determination of heavy metals because of its good selectivity, cost effectiveness, compactness and the ability for accurate simultaneous determination elements at trace levels [3]. Modified electrodes have noticeable advantages in the water heavy metals determinations. Introducing specific binding groups as thiol or cyano groups accelerate the rate of electron transfer rate at the surface of the electrode and increase the efficiency of preconcentration [4].

Silver (Ag) is regarded as the most inexpensive element among noble metals. Its unique optoelectronic properties and stability, make it has a versatile candidate to be utilized for the fabrication of polymer nanocomposites [5]. Ag shows excellent characteristics for detection of Cd and Pb with high repeatability and stability without any requirement for pretreatment, in addition to lower limits of detection (LOD) [6].

In this field of environmental monitoring, the application of nanoparticles (NPs) as a functional probe for analyzing inorganic and organic pollutants in water has been extensively studied [7, 8]. NPs usually exhibit unique characteristics rather than bulk-sized materials, principally due to the electron

Electronic supplementary material The online version of this article (<https://doi.org/10.1007/s00604-019-3552-0>) contains supplementary material, which is available to authorized users.

✉ Khalid M. Hassan
drkhalidhassan73@gmail.com

¹ Electrochemistry Research Laboratory, Physics and Mathematics Engineering Department, Faculty of Electronic Engineering, Menoufia University, Menouf 23952, Egypt

² Electrochemistry Laboratory, Chemistry Department, Faculty of Science, Menoufia University, Shibin El-Kom 32511, Egypt

confinement of the NPs [9]. From a sensing standpoint, the smaller size of them results in large aspect ratio, surface-to-volume, which lead to quick responses with high sensitivity. In addition, the optoelectronic and magnetic properties of NPs can be adjusted via manage its particle size, composition, morphology and the surface chemistry, to produce highly functional molecular probes [10].

Ag NP modified surfaces are substantial to improve optical and electrochemical characteristics and applications of potential such as catalytic and electro catalytic materials [11]. Therefore, the means of Ag NPs deposition have been widely investigated [12]. Besides the chemical methods, the electrochemical double-pulse method has previously disclosed the successful dispersion of Ag NPs on an ITO surface [13]. Though, the particle size and the distributed density of Ag NPs are highly reliant on the methods of preparations [14].

In the present work, Ag NPs were successfully deposited onto poly(1,8-diaminonaphthalene)/glassy carbon (p-1,8-DAN/GC) modified electrode by cyclic voltammetry (CV) technique. The modified silver nanoparticles/p-1,8-DAN/GC (AgNPs@p-1,8-DAN/GC) electrode was assessed towards individual and simultaneous electrochemical determination of heavy metal ions such as lead (II) (Pb^{2+}), cadmium (II) (Cd^{2+}), and copper (II) (Cu^{2+}) in 0.1 M acetate buffer solution (ABS) adjusted at pH value of 4.6 using anodic stripping voltammetry (ASV) technique. To the best of our knowledge, this is the first nanoprobe composed of an organic polymer and Ag NPs as a new green electrode material.

Experimental

Materials

1,8-Diaminonaphthalene (1,8-DAN) (Aldrich, <https://www.sigmaaldrich.com>), sulphuric acid (H_2SO_4) (Merck, <https://www.merckmillipore.com>) (98%), acetonitrile (CH_3CN) (ACN) (99.9%) HPLC (LAB-SCAN, <http://www.hurstscientific.com.au/chemicals/labscan.html>), ethanol ($\text{CH}_3\text{CH}_2\text{OH}$) (ADWIC, <https://www.nasrpharma.com/index.html>) (96%) and diamond paste (Presi) were used as received. Sodium acetate (CH_3COONa), acetic acid (CH_3COOH), silver nitrate (AgNO_3), potassium nitrate (KNO_3), lead nitrate ($\text{Pb}(\text{NO}_3)_2$), cadmium chloride (CdCl_2) and copper chloride (CuCl_2) were of analytical grade.

0.1 M ABS (pH = 4.6) was performed by addition of 5.4 g CH_3COONa to 2.4 mL glacial CH_3COOH (0.1 M) and diluted with distilled H_2O until 100.0 mL.

Instruments

A potentiostat voltammetric analyzer (BioAnalytical System (BAS)) was utilized for electrochemical measurements using

CV-50w software. All obtained voltammograms were performed in a conventional three-electrode cell composed of 3.0 mm GC (working), a platinum wire (auxiliary) and Ag/AgCl (reference) electrodes. Working electrode cleaning was accomplished by its polishing with diamond paste, rinsing in ethanol followed by used solvents.

Morphology and composition of the modified electrode surface were studied using field emission scanning electron microscopy (FE-SEM) and energy dispersive x-ray (EDX) techniques by a JEOL JSM-7001F operating at 120 kV. An Agilent 5420 atomic force microscope (AFM) was used to study the film hardness and its topography. The measurements of transmission electron microscopy (TEM) were achieved via Joel JEM 1230 with CCD camera (USC1000, Gatan Inc.) operating at 100kv. X-ray diffraction (XRD) measurements were carried on a Bruker, D8 ADVANCE X-ray powder diffractometer (range: 20–80°). X-ray photoelectron spectroscopy (XPS) was performed by using model thermo ESCA Lab 250xi. For its calibration, the binding energy was calibrated to the C 1 s line at 284.6 eV as a reference.

River samples were analyzed by inductively coupled plasma optical emission spectrometry (ICP-OES).

Electrochemical preparation of the p-1,8-DAN-modified glassy carbon electrode

P-1,8-DAN/GC modified electrode was prepared by electro polymerization of 1.0 mM 1,8-DAN in a mixed solvent of 4.5 M H_2SO_4 in ACN with a volume ratio of (1: 3) at GC electrode, for which 2.50 mL of H_2SO_4 was added to 7.50 mL of ACN to complete a total volume of 10.0 mL. This system was subjected to CV technique with potential range of +0.2 to +1.2 V at scan rate of 0.1 $\text{V} \cdot \text{s}^{-1}$ for 20 cycles as described in our previous work [15].

Electrodeposition of Ag NPs onto p-1,8-DAN film

Different techniques for electrodeposition of Ag NPs onto p-1,8-DAN film was conducted such as pulse voltammetry (PV), double pulse voltammetry (DPV), in situ procedure (Ag^+ ions in situ), and CV protocol. Firstly, PV was performed at p-1,8-DAN/GC modified electrode in 25.0 mL of aqueous solution of 0.01 M potassium nitrate (KNO_3) containing 0.01 M AgNO_3 for which a potential of -0.8 was applied with accumulation time of 300 s for Ag deposition. DPV technique was conducted in two steps at p-1,8-DAN/GC modified electrode in the previously mentioned solution (in the last point). The first step was nucleation pulse at an applied potential of +0.13 V for 50 s, and the second step was growth pulse at an applied potential of +0.24 V for 120 s. Secondly, Ag NPs electrodeposition was achieved in situ (Ag^+ ions in

situ) for which 0.01 M AgNO_3 (0.0169 g) was added to 10.0 mL of the polymerization mixed solvent (4.5 M H_2SO_4 in ACN) system during the electro polymerization process of 1.0 mM 1,8-DAN monomer using CV technique with scan rate of $0.1 \text{ V} \cdot \text{s}^{-1}$ at potential range of +0.2 to +1.2 V for 20 cycles. Final technique was performed by CV protocol by cycling a freshly prepared p-1,8-DAN/GC electrode in a solution of 0.01 M potassium nitrate (KNO_3) containing 0.01 M AgNO_3 in a potential range from -0.9 to $+0.6$ V at a scan rate $0.05 \text{ V} \cdot \text{s}^{-1}$ for 2 cycles [16]. Based on anodic peaks currents of electrochemical responses (using CV technique at scan rate $0.05 \text{ V} \cdot \text{s}^{-1}$) of different $\text{AgNPs}@p\text{-}1,8\text{-DAN/GC}$ modified electrodes prepared by different techniques in 0.1 M ABS, CV technique was chosen as it showed the highest and favorable current response (figure not shown).

Results and discussion

Analytical parameters for Ag NP electrodeposition

P-1,8-DAN film thickness was controlled using different number of polymerization cycles from 5 to 25 cycles. Film thickness performed using 20 cycles arises to give the favorable electrochemical response in ABS using CV technique at scan rate $0.05 \text{ V} \cdot \text{s}^{-1}$ in the potential range -0.9 to $+0.6$ V (vs. Ag/AgCl) (Fig. S1 A). For studying the effect of Ag^+ ions concentration, p-1,8-DAN/GC electrode was immersed in different AgNO_3 concentrations (0.1, 0.5, 1.0, 5.0, and 10.0 mM) for which the corresponding current responses were measured. Fig. S1 B indicated that the current response of $\text{AgNPs}@p\text{-}1,8\text{-DAN/GC}$ increases gradually as Ag^+ concentration raised from 0.1 to 10.0 mM. Number of cycles of Ag electrodeposition was also studied by scanning p-1,8-DAN/GC electrode in Ag^+ solution using different cycles like 2, 3, 5, 10, and 15 cycles giving the optimum results for 2 cycles (Fig. S1 C). Optimum conditions for Ag^+ electrodeposition were detected by applying CV technique to p-1,8-DAN/GC electrode (formed by 20 cycles) in a solution of 0.01 M KNO_3 containing 0.01 M AgNO_3 in the potential range from -0.9 to $+0.6$ V with scan rate of $0.05 \text{ V} \cdot \text{s}^{-1}$ for 2 cycles. (figure not shown) [16].

Figure 1 shows the electrochemical responses of p-1,8-DAN/GC and $\text{AgNPs}@p\text{-}1,8\text{-DAN/GC}$ modified electrodes in ABS using square wave voltammetry (SWV) technique in the potential range from -0.9 V to $+0.3$ V. No electrochemical response was detected at p-1,8-DAN/GC electrode (Fig. 1a). The modified electrode has a well-defined anodic peak appeared at $+0.45$ V for Ag^+ ions stripping with an anodic peak current of $49.0 \mu\text{A}$ (Fig. 1b). This indicates that the working potential window from -0.9 V to 0.0 V is suitable for the studied heavy metal ions determination. The wide-range

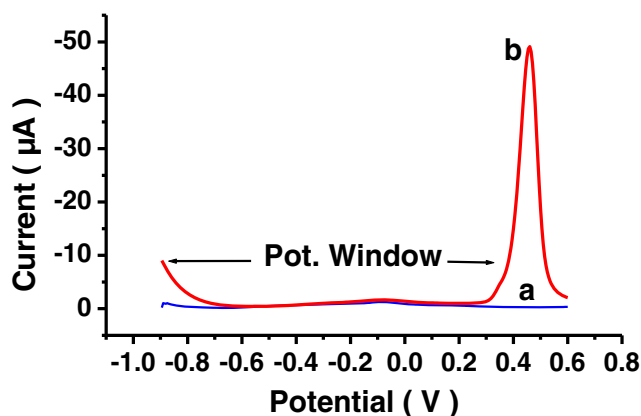


Fig. 1 Square wave voltammograms of: (a) p-1,8-DAN/GC and (b) $\text{AgNPs}@p\text{-}1,8\text{-DAN/GC}$ electrodes in ABS using scan rate of $0.005 \text{ V} \cdot \text{s}^{-1}$, time duration of 1 s and amplitude of 0.025 V in the potential range -1.0 to $+0.6$ V (vs. Ag/AgCl)

potential space offers a pronounced improvement of the electrode applications for ASV of heavy metals.

Surface and bulk characterization of $\text{AgNPs}@p\text{-}1,8\text{-DAN}$ -modified glassy carbon electrode

Characterization of $\text{AgNPs}@p\text{-}1,8\text{-DAN}$ -modified electrode was carried out using different techniques like FE-SEM, EDX, XPS and AFM (for surface analysis), while XRD and TEM (for bulk analysis). FE-SEM is employed to characterize the surface morphology of the electrode. Figure 2a shows a rough grayish black surface indicative for the presence of p-1,8-DAN/GC electrode. SEM image (Fig. 2b) indicates a homogenous dispersion of Ag NPs at p-1,8-DAN/GC surface. Furthermore, EDX experiments confirm the Ag deposition giving signals corresponding to Ag metal with a percentage of 97.4% (Fig. 2c).

TEM image represents the morphology of Ag NPs almost as a spherical in shape (Fig. 2 D) for which the particles size ranges from 10.0 nm to 60.0 nm with an average size around 35.5 nm as shown in Fig. 2c inset (diameter distribution histogram).

The crystallinity of Ag NPs was studied by XRD pattern for which diffractions peaks appeared at 38.3° , 44.25° , 64.72° , and 77.40° which are related to the (111), (200), (220), and (311) planes of Ag face-centered cubic, respectively (Fig. 3a) [17]. The strongest diffraction that arises from the (111) plane is a characteristic of such phase. The crystallite size was determined from the full-width at half maximum (FWHM) of the highest reflection of the (111) peak at $2\theta = 38.3^\circ$. Determined crystallite size came out to be 39 nm.

Surface elemental analysis via XPS enabled further insight into the composition of the $\text{AgNPs}@p\text{-}1,8\text{-DAN/GC}$

Fig. 2 **a** FE-SEM image of p-1,8-DAN/GC electrode, **b** FE-SEM image of AgNPs@p-1,8-DAN/GC electrode, **c** EDX for the surface of AgNPs@p-1,8-DAN/GC electrode and **d** TEM image of Ag NPs (inset: diameter distribution histogram)

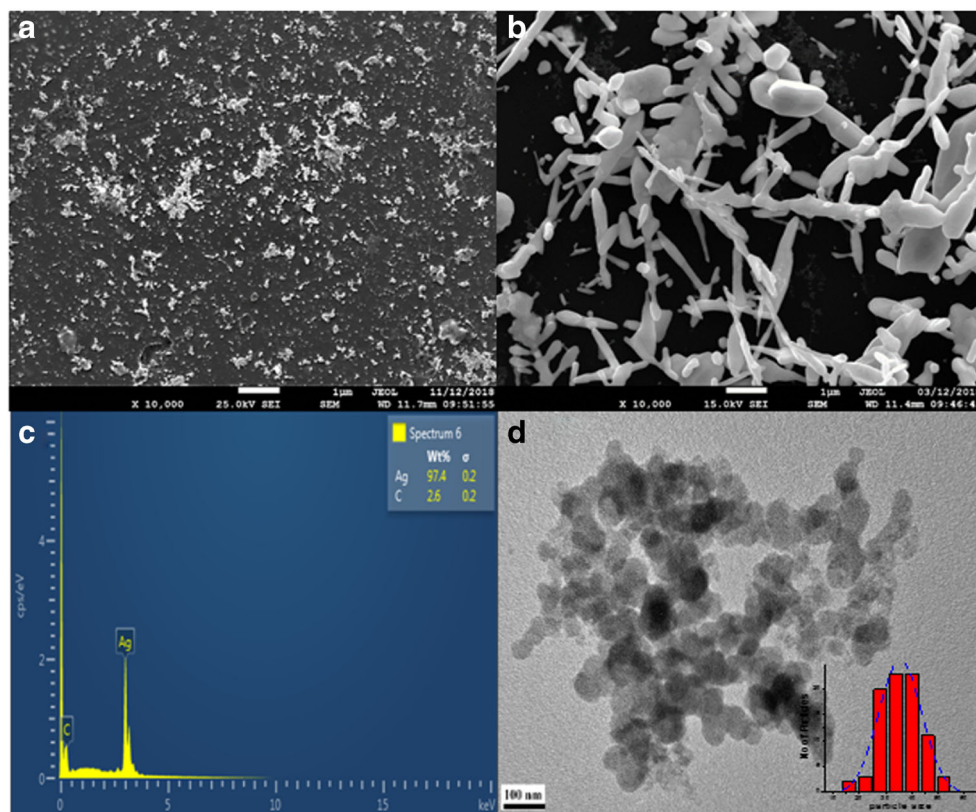
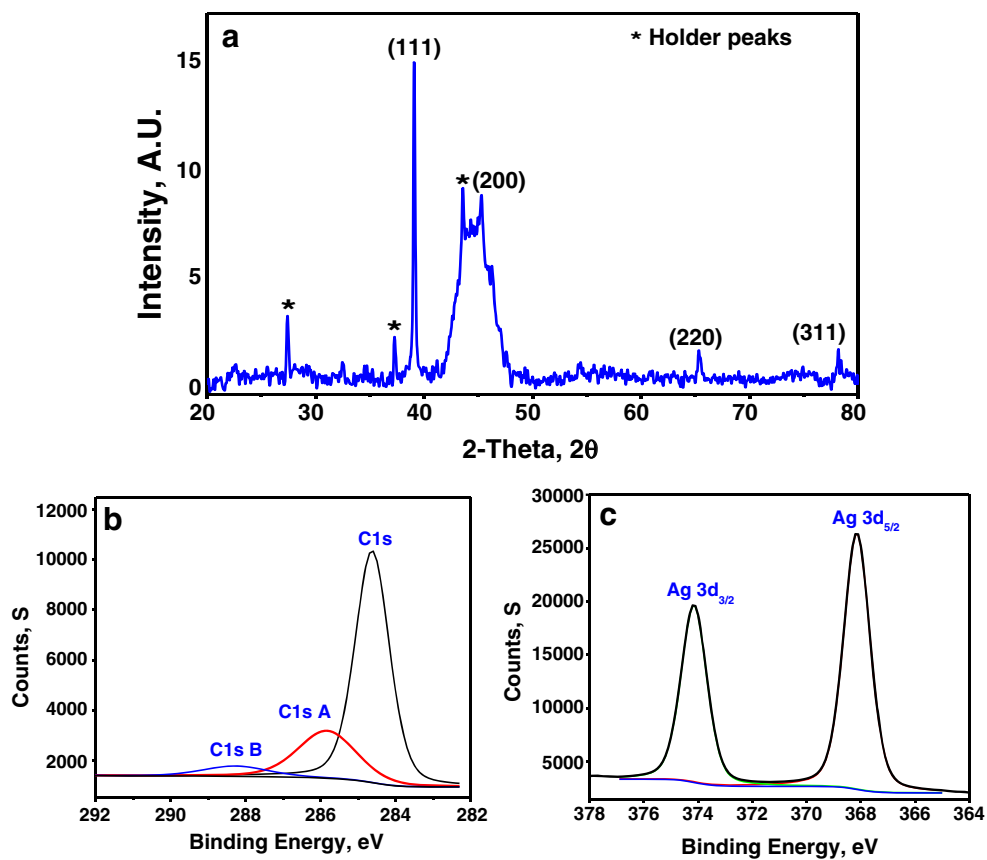


Fig. 3 **a** XRD pattern, **b** Deconvoluted XPS for C1s, and **c** Deconvoluted XPS for Ag_{3d} of AgNPs@p-1,8-DAN/GC modified electrode



electrode surface. The modified electrode surface showed the presence of carbon, silver and nitrogen elements (not shown). The presence of three components in C1s high resolution region at 284.6, 285.8, and 288.2 eV (Fig. 3b) are ascribed to C–C, C–N, and amide bonding in the p-1,8-DAN film, respectively. For determination of the chemical environment and oxidation state of Ag NPs, XPS measurements were carried out at the Ag 3d core levels. Figure 3c displays the spectrum Ag 3d involves two peaks at 374.15 and 368.15 eV, which are attributed to binding energies for Ag 3d_{3/2} and Ag 3d_{5/2} of metallic Ag, respectively. Results are in good approval with other results which obtained from XRD which implies the presence of pure metallic Ag NPs.

Electrodes surfaces were visualized using tapping mode AFM. The root-mean-square (rms) roughness values were evaluated from 3D image topographies of p-1,8-DAN/GC and AgNPs@p-1,8-DAN/GC modified electrodes surfaces with 5.6 nm and 15.9 nm, respectively (Fig. 4a and b). Also, small protuberant peaks which were detected in 2D and 3D AFM images of the nanoprobe electrode surface confirming the successful deposition of Ag NPs on the electrode.

Electrochemical behavior and effective surface area of AgNPs@p-1,8-DAN-modified glassy carbon electrode

The electrochemical behaviors of GC, p-1,8-DAN/GC and AgNPs@p-1,8-DAN/GC electrodes were examined in 2.0 mM potassium ferrocyanide (K₄[Fe (CN)₆]) in 0.10 M KCl aqueous solution using CV technique as illustrated in Fig. S2 (a, b and c). Peak-to-peak separation (ΔE_p) values were recorded at 0.93, 0.12 and 0.011 V for the three electrodes, respectively with increasing of peak current of AgNPs@p-1,8-DAN/GC electrode due to the presence of Ag NPs. The low ΔE_p for the previous electrode (nanoprobe) indicates a fast electron transfer higher than both GC and p-1,8-DAN/GC electrodes. This means that introducing Ag NPs at the surface of p-1,8-DAN/GC electrode develops its electrochemical performance.

The effective surface areas of p-1,8-DAN/GC and AgNPs@p-1,8-DAN/GC electrodes were calculated using Randles-Sevcik equation for a reversible process in [Fe (CN)₆]^{3-/4-} [18] as presented in Eq. 1:

$$I_p = 2.69 \times 10^5 D^{1/2} n^3/2 A v^{1/2} C \quad (1)$$

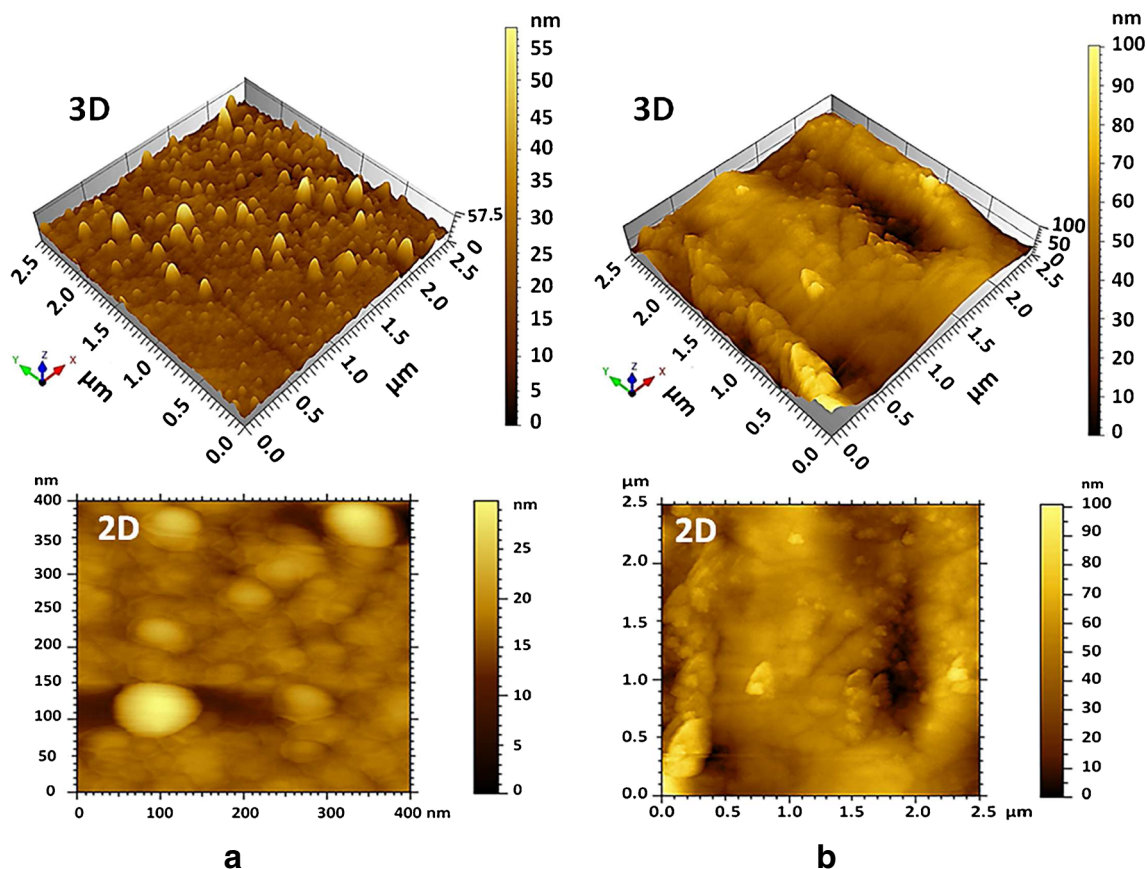


Fig. 4 AFM images of 3D and 2D of (a) p-1,8-DAN/GC, and (b) AgNPs@p-1,8-DAN/GC modified electrodes

where A (effective surface area of electrode), D (diffusion coefficient of $[\text{Fe}(\text{CN})_6]^{3-/4-}$ equal $7.6 \times 10^{-5} \text{ cm}^2 \text{ s}^{-1}$), C (bulk concentration of redox probe $[1.0 \text{ mM } [\text{Fe}(\text{CN})_6]^{3-/4-}]$), n (number of transferred electrons in $[\text{Fe}(\text{CN})_6]^{3-/4-}$ and equals equal one). The effective surface area of p-1,8-DAN/GC electrode was found to be 0.1311 cm^2 . The surface area increased by about 5 times when Ag NPs incorporated into p-1,8-DAN film to reach 0.5536 cm^2 .

Electrochemical determination of individual Pb^{2+} , Cd^{2+} and Cu^{2+} heavy metal ions

The electrochemical determination of $10.0 \mu\text{M}$ Cd^{2+} ions in ABS at both GC and p-1,8-DAN/GC electrodes using ASV technique with accumulation time 120 s and scan rate of $0.005 \text{ V} \cdot \text{s}^{-1}$ were not detected (Fig. S3 A, a and b). At AgNPs@p-1,8-DAN/GC modified electrode, an anodic peak appeared at -0.98 V with an anodic peak current of $4.31 \mu\text{A}$ (Fig. S3 A, c). The electrochemical determination of $10.0 \mu\text{M}$ Pb^{2+} ions at the three electrodes were examined (Fig. S3 B). No peaks were detected at GC electrode (Fig. S3 B, a). Two anodic peaks appeared at -0.77 V and -0.82 V with anodic peak currents of $3.6 \mu\text{A}$ and $7.2 \mu\text{A}$ were detected for both p-1,8-DAN/GC and AgNPs@P-1,8-DAN/GC electrodes, respectively with a favorable higher value for the last electrode (Fig. S3 B, b and c). The anodic stripping voltammograms in Fig. S3 C illustrates the ability of GC electrode and p-1,8-DAN/GC electrode to detect $25.0 \mu\text{M}$ of Cu^{2+} ions at -0.27 V and -0.23 V with anodic peaks currents of $0.4 \mu\text{A}$ and $8.4 \mu\text{A}$, respectively (Fig. S3 C a and b). AgNPs@p-1,8-DAN/GC modified electrode showed more sensitivity as indicated by higher anodic peak current value to reach $11.9 \mu\text{A}$ at -0.29 V (Fig. S3 C c).

Previous results indicated that Pb^{2+} and Cu^{2+} ions can be detected individually at p-1,8-DAN/GC electrode while Cd^{2+} ions were not detected. This can be correlated to the presence of amine/imine function groups acting as chelating sites with for Pb^{2+} and Cu^{2+} ions [19]. On the other hand, the three ions were detected at AgNPs@P-1,8-DAN nanoprobe with peak potentials -0.82 V , -0.29 V and -0.98 V , respectively with a remarkable raise in their current. The synergistic contributions from both P-1,8-DAN and Ag NPs improve the accumulation efficiency and the rate of charge transfer of the metal ions throughout ASV analysis. Additionally, Ag creates fused alloys with several heavy metals making it more readily to be reduced [19]. Such Ag alloys facilitated the nucleation process during heavy metal depositions in a similar manner to early described by Wang for Bi electrodes [3]. This can also explain why

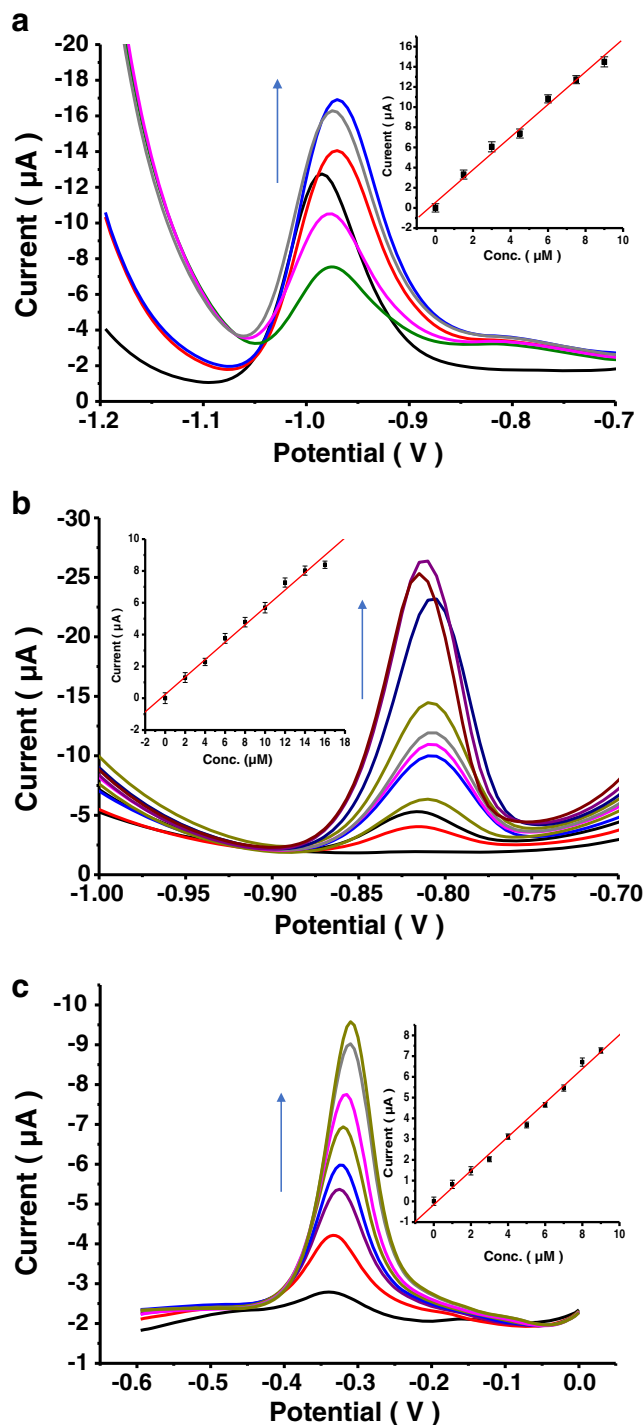
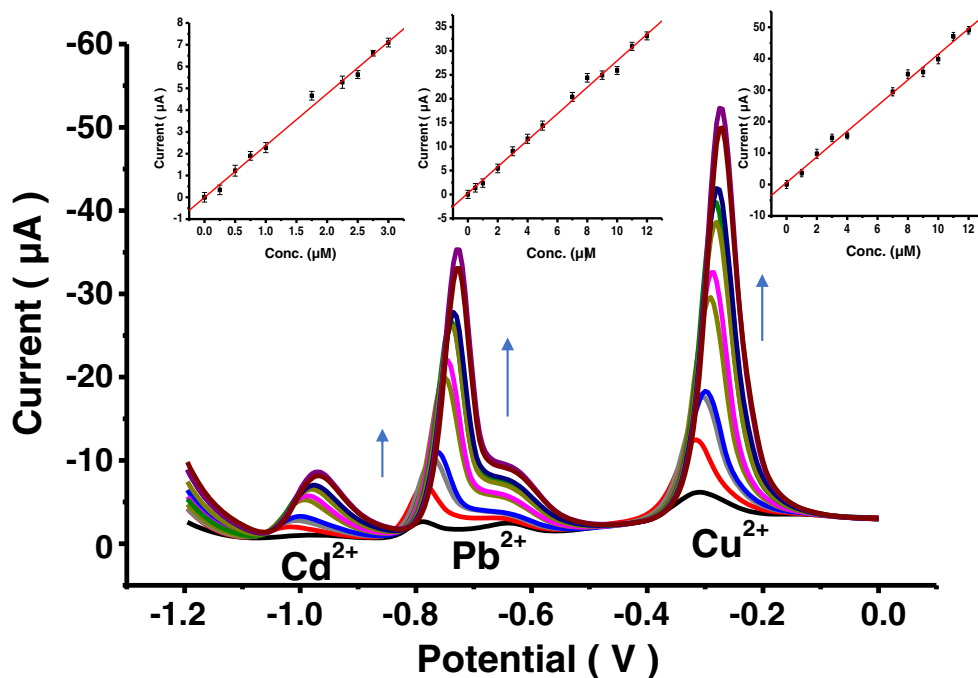


Fig. 5 Anodic stripping voltammograms of $1.5\text{--}9.0 \mu\text{M}$ for Cd^{2+} , $2.00\text{--}24.0 \mu\text{M}$ for Pb^{2+} , and $2.00\text{--}9.0 \mu\text{M}$ for Cu^{2+} in ABS at AgNPs@p-1,8-DAN/GC electrode with accumulation time 120 s, scan rate of $0.005 \text{ V} \cdot \text{s}^{-1}$ and amplitude of 0.025 V between -1.20 to 0.0 V (vs. Ag/AgCl). Insets, relations between different ions concentrations and the corresponding anodic peaks currents

Cd^{2+} ions were detected only at AgNPs@p-1,8-DAN/GC electrode.

Fig. 6 Anodic stripping voltammograms of Cd^{2+} ions concentrations (0.25–3.0 μM), Pb^{2+} and Cu^{2+} ions concentrations (1.0–12.0 μM) at $\text{AgNPs@p-1,8-DAN/GC}$ electrode in ABS with accumulation time 120 s, scan rate of $0.005 \text{ V} \cdot \text{s}^{-1}$ and amplitude of 0.025 V between -1.20 to 0.0 V (vs. Ag/AgCl). Insets, relations between different ions concentrations and the corresponding anodic peaks currents



Effect of individual heavy metal Pb^{2+} , Cd^{2+} and Cu^{2+} ions concentrations

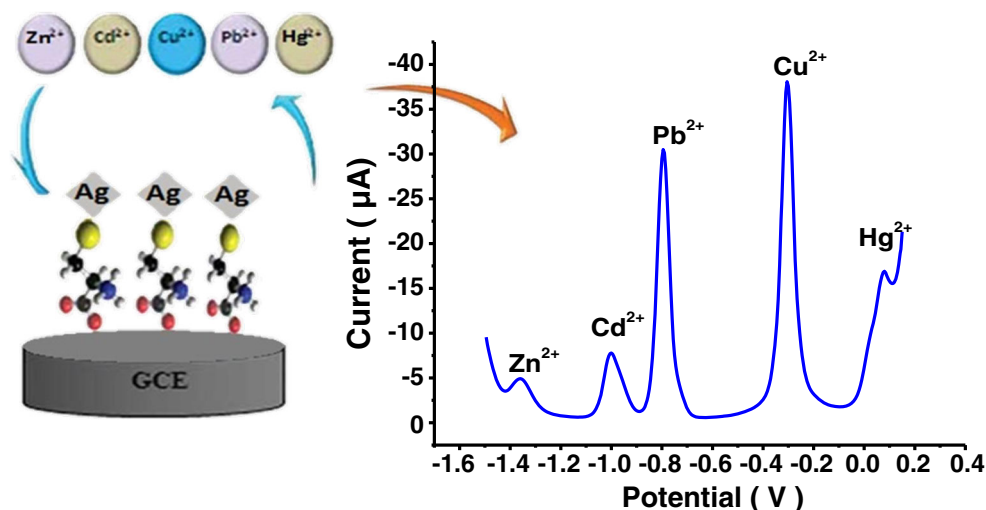
Individual determination of low concentrations of different heavy metal ions were studied between -1.20 to 0.0 V (vs. Ag/AgCl) at ranges like: $0.90 \text{ nM} - 9.0 \mu\text{M}$ for Cd^{2+} , $2.0 \text{ nM} - 24.0 \mu\text{M}$ for Pb^{2+} , and $1.3 \text{ nM} - 9.0 \mu\text{M}$ for Cu^{2+} , while the presented data are in the concentration windows of $1.5\text{--}9.0 \mu\text{M}$ for Cd^{2+} , $2.00\text{--}24.0 \mu\text{M}$ for Pb^{2+} , and $2.00\text{--}9.0 \mu\text{M}$ for Cu^{2+} . Figure 5a, b and c represents the anodic stripping voltammograms recorded at $\text{AgNPs@p-1,8-DAN/GC}$ electrode with accumulation time 120 s and scan rate of $0.005 \text{ V} \cdot \text{s}^{-1}$, while Fig. 5 insets, represent the relation between different ions concentrations (in all ranges) and the corresponding anodic peaks

currents. The anodic stripping peak currents were raised linearly upon increasing the concentrations of the studied metal ions. The calculated correlation coefficients (R^2), LOD and limit of quantification (LOQ) are collected in Table S1 indicating the high sensitivity of the modified electrode towards the three heavy metal ions individual determination.

Simultaneous electrochemical determination of Pb^{2+} , Cd^{2+} , and Cu^{2+} heavy metal ions in a ternary mixture

The goal of this work is to detect Cd^{2+} , Pb^{2+} , and Cu^{2+} ions simultaneously. Anodic stripping voltammograms of a mixture of $0.5 \mu\text{M}$ Cd^{2+} , $2.0 \mu\text{M}$ Pb^{2+} and $2.0 \mu\text{M}$ Cu^{2+} at p-1,8-DAN/GC and $\text{AgNPs@p-1,8-DAN/GC}$ electrodes in ABS at a scan

Fig. 7 Anodic stripping voltammograms of $0.5 \mu\text{M}$ Cd^{2+} , $2.0 \mu\text{M}$ Pb^{2+} , and $2.0 \mu\text{M}$ Cu^{2+} ions in presence of $2.0 \mu\text{M}$ Zn^{2+} and $0.5 \mu\text{M}$ Hg^{2+} ions at $\text{AgNPs@p-1,8-DAN/GC}$ electrode in ABS with accumulation time 120 s, scan rate of $0.005 \text{ V} \cdot \text{s}^{-1}$ and amplitude of 0.025 V between -1.60 to $+0.2 \text{ V}$ (vs. Ag/AgCl)



rate of $0.005 \text{ V} \cdot \text{s}^{-1}$ with accumulation time 120 s were recorded (Fig. S4 a and b). In Fig. S4 a, Cd^{2+} , Pb^{2+} and Cu^{2+} ions were simultaneously detected at p-1,8-DAN/GC electrode at -1.06 , -0.82 and 0.35 V with anodic stripping currents of $0.33 \mu\text{A}$, $1.52 \mu\text{A}$ and $3.54 \mu\text{A}$, respectively. At AgNPs@p-1,8-DAN/GC electrode (Fig. S4 b), peak potentials of Cd^{2+} , Pb^{2+} , and Cu^{2+} ions were detected at -1.02 , -0.78 and -0.32 V with anodic stripping currents of $1.22 \mu\text{A}$, $5.43 \mu\text{A}$ and $9.76 \mu\text{A}$, respectively. The remarkable differences in stripping peak potentials between Pb^{2+} , Cd^{2+} and Cu^{2+} indicated the possibility of their simultaneous detection due to the strong activity of Ag NPs decorated p-1,8-DAN film. Peak currents at AgNPs@p-1,8-DAN/GC electrode compared with p-1,8-DAN/GC electrode demonstrates the role of Ag NPs towards the enhanced responses of Pb^{2+} , Cd^{2+} , and Cu^{2+} ions.

Simultaneous determination of different concentrations of studied heavy metal ions were studied in the voltage range from -1.20 to 0.0 V (vs. Ag/AgCl) at low concentrations ranges like: $0.15 \text{ nM} - 3.0 \mu\text{M}$ for Cd^{2+} , $0.13 \text{ nM} - 12.0 \mu\text{M}$ for Pb^{2+} , and $0.07 \text{ nM} - 12.0 \mu\text{M}$ for Cu^{2+} , while an ASVs of several Cd^{2+} ions concentrations ($0.25\text{--}3.0 \mu\text{M}$), Pb^{2+} and Cu^{2+} ions concentrations ($1.0\text{--}12.0 \mu\text{M}$) in ABS at AgNPs@p-1,8-DAN/GC are presented in Fig. 6. Stripping peaks were appeared at -0.98 , -0.74 and -0.28 V for Cd^{2+} , Pb^{2+} and Cu^{2+} , respectively. It is important to mention that at the higher concentration like $1.0 \mu\text{M}$, a second stripping peak appeared for Pb^{2+} ions. As the concentration was increased further, the magnitude of this second peak was also found to increase as presented in literature [20].

Figure 6 insets, represent the relation between different ions concentrations (in all ranges) and the corresponding anodic peaks currents. Results reveal that the anodic stripping peaks heights of all the studied heavy metal ions improved linearly with increasing their concentrations.

The resulting calibration plots exhibited an excellent linearity of current dependence for their corresponding concentrations with R^2 values of 0.9938 for Cd^{2+} , 0.9946 for Pb^{2+} , and 0.9934 for Cu^{2+} . LOD values were estimated to be 0.17 nM , 0.15 nM and 0.09 nM for Cd^{2+} , Pb^{2+} , and Cu^{2+} ions, respectively as collected in Table S2. As represented, the nanoprobe is highly sensitive for simultaneous determination of Cd^{2+} , Pb^{2+} , and Cu^{2+} ions in ternary mixture with lower LOD and LOQ values.

Repeatability

Repeatability was evaluated by six times successive determination of $0.5 \mu\text{M}$ Cd^{2+} , $2.0 \mu\text{M}$ Pb^{2+} and $2.0 \mu\text{M}$ Cu^{2+} ions at the same nanoprobe by recording their peak responses (Fig. S5). The nanoprobe exhibited good repeatability and stability due to the high adsorption between Ag NPs and Cd^{2+} , Pb^{2+} and Cu^{2+} ions [21].

Interference studies

Interferences of additional metal ions were examined for evaluating the ability of the nanoprobe for determination of Cd^{2+} , Pb^{2+} , and Cu^{2+} ions in presence of zinc (II) (Zn^{2+}) and

Table 1 Comparison of analytical performance of AgNPs@p-1,8-DAN/GC modified electrode with other similar systems

Electrode substrate	Measurement technique	Medium	Limits of detection ($\mu\text{g} \cdot \text{L}^{-1}$)			Ref.
			Cd^{2+}	Pb^{2+}	Cu^{2+}	
MWCNT/P1,5-DAN	ASV	ABS pH 4.5	3.20	2.10	–	[22]
RGO-CS/PLL/GCE	DPASV	ABS pH 4.5	0.01	0.02	0.02	[23]
Bi/CNT/GCE	ASV	ABS pH 4.5	0.70	1.30	–	[24]
Bi/CNT/SPE	ASV	ABS pH 4.5	0.80	0.20	–	[25]
Hg-Bi /SWNTs/GCE	ASV	KCl+ ABS pH 6.0	0.076	0.18	–	[26]
Bi/Graphene/MWCNT/GCE	DPASV	ABS pH 4.5	0.10	0.20	–	[27]
Bi/Nafion/Graphene/GCE	DPASV	ABS pH 4.5	0.02	0.02	–	[28]
Bi/EG/PG	ASV	ABS pH 4.6	0.10	0.13	–	[29]
Pt/MWCNT/P1,5-DAN electrode	ASV	ABS pH 4.5	2.10	3.20	–	[22]
GCE-MWCNT/poly (PCV)/Bi	DPASV	ABS pH 5.0	0.20	0.40	–	[30]
CB-18-crown-6-GEC	DPASV	ABS pH 4.5	2.40	1.50	1.50	[31]
RGO/Bi/CPE	DPASV	ABS pH 5.5	2.80	0.55	26.0	[32]
GC/CNT/nanoAu-SiO ₂	DPASV	HCl	–	0.47	0.34	[33]
Ag-bipy-CP/PMB/GCE	DPV	ABS pH 5.0	–	2.30	0.71	[34]
AgNPs/RGO	ASV	ABS pH 5.0	$0.254 \mu\text{M}$	$0.141 \mu\text{M}$	$0.178 \mu\text{M}$	[35]
AgNPs@P-1,8-DAN/GC	ASV	ABS pH 4.6	0.019 (0.17 nM)	0.031 (0.15 nM)	0.005 (0.09 nM)	This work

mercury (II) (Hg^{2+}) ions. Interference studies performed using ASV technique with accumulation time 120 s and a scan rate of $0.005 \text{ V} \cdot \text{s}^{-1}$ by addition of $2.0 \mu\text{M Zn}^{2+}$ and $0.5 \mu\text{M Hg}^{2+}$ ions into the ABS containing $0.5 \mu\text{M Cd}^{2+}$, $2.0 \mu\text{M Pb}^{2+}$, and $2.0 \mu\text{M Cu}^{2+}$ ions. Well-defined sharp peaks of Cd^{2+} , Pb^{2+} , and Cu^{2+} were observed as illustrated in Fig. 7. The presence of both Zn^{2+} and Hg^{2+} ions did not affect peak responses for other ions with working voltages of -1.36 and $+0.9 \text{ V}$, respectively. The high surface area of Ag NPs supports high sensitivity for heavy metals ions detection and diminishes the interference for their simultaneously determination devoid of losing response intensities.

Real sample determination

The nanoprobe was tested in tap water collected and adjusted with ABS for estimating its performance. Neither Cd^{2+} , Pb^{2+} nor Cu^{2+} traces were found (Fig. S6 a). Then, typical addition method had been used as an identified quantity were spiked into the water sample (of the previous ions) and ASV responses were examined with accumulation time 120 s and scan rate of $0.005 \text{ V} \cdot \text{s}^{-1}$ (Fig. S6 b). It was found that the electrode can successfully determine simultaneously Cd^{2+} , Pb^{2+} and Cu^{2+} ions in tap water with high sensitivity. Table S3 optimizes the recoveries for results which obtained for two samples in absence and presence of spiked heavy metal ions. Results show high recoveries between 103.0% and 108.0%. Good results detected in recovery procedure indicated that the investigated AgNPs@p-1,8-DAN/GC electrode is suitable for the simultaneously determination of Cd^{2+} , Pb^{2+} and Cu^{2+} ions in real water samples.

To further demonstrate the practicality of the present electrode, study also evaluated the simultaneous determination of Cd^{2+} , Pb^{2+} , and Cu^{2+} ions in contaminated three river water samples. The stripping signals of all studied ions were all observed with the presented nanoprobe with high good recoveries and confirmed by means of comparison with data obtained from ICP-OES method as presented in Table S4.

Electrochemical performance of the nanoprobe was compared with parallel systems in literatures used for the electrochemical determination of Cd^{2+} , Pb^{2+} and Cu^{2+} ions (Table 1). Comparisons showed that the AgNPs@p-1,8-DAN/GC modified electrode can be a promising nanoprobe to be used for the determination of these heavy metal ions individually and simultaneously with high sensitivity and low LOD values.

Conclusion

The advantageous features of AgNPs@p-1,8-DAN/GC modified electrode have been revealed, this new nanoprobe was fabricated by electro polymerization method and Ag NPs were

electrodeposited onto p-1,8-DAN film by CV technique and characterized via different surface and bulk analytical techniques. The AgNPs@p-1,8-DAN/GC modified electrode used for individual and simultaneous determination of Cd^{2+} , Pb^{2+} and Cu^{2+} ions in ABS using ASV technique with high sensitivity and low values of LOD and LOQ. Additionally, it can detect other heavy metal ions like Zn^{2+} and Hg^{2+} in the same system. The presented nanoprobe exhibited highly electrocatalytic activity compared to the previous electrodes for electrochemical determination of these ions and the performance of the electrode shows high stability and sensitivity beside selectivity.

Acknowledgements The authors are appreciative to Alexander von Humboldt Foundation for providing some electrodes and accessories.

Compliance with ethical standards The author(s) declare that they have no competing interests.

References

1. El Mhammedi MA, Achak M, Bakasse M (2013) Evaluation of a platinum electrode modified with hydroxyapatite in the lead (II) determination in a square wave voltammetric procedure. *Arab J Chem* 6(3):299–305. <https://doi.org/10.1016/j.arabjc.2010.10.010>
2. Pohl P (2009) Determination of metal content in honey by atomic absorption and emission spectrometries. *Trends Anal Chem* 28(1): 117–128. <https://doi.org/10.1016/j.trac.2008.09.015>
3. Wang J (2005) Stripping analysis at bismuth electrodes: a review. *Electroanal* 17(15–16):1341–1346. <https://doi.org/10.1002/elan.200403270>
4. Su Z, Liu Y, Zhang Y, Xie Q, Chen L, Huang Y, Fu Y, Meng Y, Li X, Ma M, Yao S (2013) Thiol–ene chemistry guided preparation of thiolated polymeric nanocomposite for anodic stripping voltammetric analysis of Cd^{2+} and Pb^{2+} . *Analyst* 138(4):1180–1186. <https://doi.org/10.1039/C2AN36114K>
5. Tang J, Li Z, Xia Q, Williams RS (2009) Fractal structure formation from Ag nanoparticle films on insulating substrates. *Langmuir* 25(13):7222–7225. <https://doi.org/10.1021/la9010532>
6. March G, Nguyen T, Piro B (2015) Modified electrodes used for electrochemical detection of metal ions in environmental analysis. *Biosens* 5(2):241–275. <https://doi.org/10.3390/bios5020241>
7. Wang Z, Ma L (2009) Gold nanoparticle probes. *Coord Chem Rev* 253(11–12):1607–1618. <https://doi.org/10.1016/j.ccr.2009.01.005>
8. Cheon J, Lee J-H (2008) Synergistically integrated nanoparticles as multimodal probes for Nanobiotechnology. *Acc Chem Res* 41(12): 1630–1640. <https://doi.org/10.1021/ar800045c>
9. Berlina AN, Zherdev AV, Dzantiev BB (2019) Progress in rapid optical assays for heavy metal ions based on the use of nanoparticles and receptor molecules. *Microchim Acta* 186(3):172. <https://doi.org/10.1007/s00604-018-3168-9>
10. Hahn J-I (2013) Biomedical detection via macro- and nano-sensors fabricated with metallic and semiconducting oxides. *J Biomed Nanotechnol* 9(1):1–25. <http://www.ncbi.nlm.nih.gov/pmc/articles/PMC3766318/>
11. Nishijo J, Oishi O, Judai K, Nishi N (2007) Facile and mass-producible fabrication of one-dimensional ag nanoparticle arrays. *Chem Mater* 19(19):4627–4629. <https://doi.org/10.1021/cm071688i>

12. Zheng J, Li X, Gu R, Lu T (2002) Comparison of the surface properties of the assembled silver nanoparticle electrode and roughened silver electrode. *J Phys Chem B* 106(5):1019–1023. <https://doi.org/10.1021/jp012083r>
13. Sandmann G, Dietz H, Plieth W (2000) Preparation of silver nanoparticles on ITO surfaces by a double-pulse method. *J Electroanal Chem* 491(1–2):78–86. [https://doi.org/10.1016/S0022-0728\(00\)00301-6](https://doi.org/10.1016/S0022-0728(00)00301-6)
14. Xing S, Xu H, Chen J, Shi G, Jin L (2011) Nafion stabilized silver nanoparticles modified electrode and its application to Cr (VI) detection. *J Electroanal Chem* 652(1–2):60–65. <https://doi.org/10.1016/j.jelechem.2010.03.035>
15. Hassan K, Abdel Azzem M (2015) Electrocatalytic oxidation of ascorbic acid, uric acid, and glucose at nickel nanoparticles/poly (1-amino-2-methyl-9,10-anthraquinone) modified electrode in basic medium. *J Appl Electrochem* 45(6):567–575. <https://doi.org/10.1007/s10800-015-0805-4>
16. Ng KH, Liu H, Penner RM (2000) Subnanometer silver clusters exhibiting unexpected electrochemical Metastability on graphite. *Langmuir* 16(8):4016–4023. <https://doi.org/10.1021/la9914716>
17. Shameli K, Ahmad MB, Jazayeri SD, Shabanzadeh P, Sangpour P, Jahangirian H, Gharayebi Y (2012) Investigation of antibacterial properties silver nanoparticles prepared via green method. *Chem Cent J* 6(1):73. <https://doi.org/10.1186/1752-153x-6-73>
18. Bard AJ, Faulkner LR (2001) Fundamentals and applications, vol 2. *Electrochemical Methods*
19. Salih FE, Ouarzane A, El Rhazi M (2017) Electrochemical detection of lead (II) at bismuth/poly(1,8-diaminonaphthalene) modified carbon paste electrode. *Arab J Chem* 10(5):596–603. <https://doi.org/10.1016/j.arabjc.2015.08.021>
20. Hutton LA, Newton ME, Unwin PR, Macpherson JV (2011) Factors controlling stripping voltammetry of Lead at polycrystalline boron doped diamond electrodes: new insights from high-resolution microscopy. *Anal Chem* 83(3):735–745. <https://doi.org/10.1021/ac101626s>
21. Hassan KM, Elsaid Gaber S, Fatehy M, Abdel Azzem M (2018) Novel sensor based on poly (1,2-Diaminoanthraquinone) for individual and simultaneous anodic stripping voltammetry of Cd²⁺, Pb²⁺, Cu²⁺ and Hg²⁺. *J Electroanal* 30(6):1155–1162. <https://doi.org/10.1002/elan.201800097>
22. Vu HD, Nguyen L-H, Nguyen TD, Nguyen HB, Nguyen TL, Tran DL (2015) Anodic stripping voltammetric determination of Cd²⁺ and Pb²⁺ using interpenetrated MWCNT/P1,5-DAN as an enhanced sensing interface. *Ionics* 21(2):571–578. <https://doi.org/10.1007/s11581-014-1199-8>
23. Guo Z, Li D-d, Luo X-k, Li Y-h, Zhao Q-N, Li M-m, Zhao Y-t, Sun T-s, Ma C (2017) Simultaneous determination of trace Cd (II), Pb (II) and Cu (II) by differential pulse anodic stripping voltammetry using a reduced graphene oxide-chitosan/poly-l-lysine nanocomposite modified glassy carbon electrode. *J Colloid Interface Sci* 490:11–22. <https://doi.org/10.1016/j.jcis.2016.11.006>
24. Hwang GH, Han WK, Park JS, Kang SG (2008) Determination of trace metals by anodic stripping voltammetry using a bismuth-modified carbon nanotube electrode. *Talanta* 76(2):301–308. <https://doi.org/10.1016/j.talanta.2008.02.039>
25. Wang Z, Wang H, Zhang Z, Liu G (2014) Electrochemical determination of lead and cadmium in rice by a disposable bismuth/electrochemically reduced graphene/ionic liquid composite modified screen-printed electrode. *Sensors Actuators B Chem* 199:7–14. <https://doi.org/10.1016/j.snb.2014.03.092>
26. Ouyang R, Zhu Z, Tatum CE, Chambers JQ, Xue Z-L (2011) Simultaneous stripping detection of Zn (II), Cd (II) and Pb (II) using a bimetallic Hg–Bi/single-walled carbon nanotubes composite electrode. *J Electroanal Chem* 656(1–2):78–84. <https://doi.org/10.1016/j.jelechem.2011.01.006>
27. Huang H, Chen T, Liu X, Ma H (2014) Ultrasensitive and simultaneous detection of heavy metal ions based on three-dimensional graphene-carbon nanotubes hybrid electrode materials. *Anal Chim Acta* 852:45–54. <https://doi.org/10.1016/j.aca.2014.09.010>
28. Li J, Guo S, Zhai Y, Wang E (2009) High-sensitivity determination of lead and cadmium based on the Nafion-graphene composite film. *Anal Chim Acta* 649(2):196–201. <https://doi.org/10.1016/j.aca.2009.07.030>
29. Pokpas K, Zbeda S, Jahed N, Mohamed N, Baker PG, Iwuoha EI (2014) Electrochemically reduced graphene oxide pencil-graphite in situ plated bismuth-film electrode for the determination of trace metals by anodic stripping voltammetry. *Int J Electrochem Sci* 9: 736–759. <http://hdl.handle.net/10566/3290>
30. Chamjangali MA, Kouhestani H, Masdarolomoor F, Daneshnejad H (2015) A voltammetric sensor based on the glassy carbon electrode modified with multi-walled carbon nanotube/poly(pyrocatechol violet)/bismuth film for determination of cadmium and lead as environmental pollutants. *Sensors Actuators B Chem* 216:384–393. <https://doi.org/10.1016/j.snb.2015.04.058>
31. Serrano N, González-Calabuig A, del Valle M (2015) Crown ether-modified electrodes for the simultaneous stripping voltammetric determination of Cd (II), Pb (II) and Cu (II). *Talanta* 138:130–137. <https://doi.org/10.1016/j.talanta.2015.01.044>
32. Sahoo PK, Panigrahy B, Sahoo S, Satpati AK, Li D, Bahadur D (2013) In situ synthesis and properties of reduced graphene oxide/Bi nanocomposites: As an electroactive material for analysis of heavy metals. *Biosens Bioelectron* 43:293–296. <https://doi.org/10.1016/j.bios.2012.12.031>
33. Silva ACO, Oliveira LCF, Delfino AV, Meneghetti MR, Abreu FC (2016) Electrochemical study of carbon nanotubes/Nanohybrids for determination of metal species Cu²⁺ and Pb²⁺ in water samples. *J Anal Methods Chem* 2016:1–12. <https://doi.org/10.1155/2016/9802738>
34. Chira A, Bucur B, Bucur MP, Radu GL (2014) Electrode-modified with nanoparticles composed of 4,4[prime or minute]-bipyridine-silver coordination polymer for sensitive determination of Hg (II), Cu (II) and Pb (II). *New J Chem* 38(11):5641–5646. <https://doi.org/10.1039/C4NJ01245C>
35. Sang S, Li D, Zhang H, Sun Y, Jian A, Zhang Q, Zhang W (2017) Facile synthesis of AgNPs on reduced graphene oxide for highly sensitive simultaneous detection of heavy metal ions. *RSC Adv* 7(35):21618–21624. <https://doi.org/10.1039/C7RA02267K>

Publisher's note Springer Nature remains neutral with regard to jurisdictional claims in published maps and institutional affiliations.